Clim Dyn (2009) 33:1069–1074
DOI 10.1007/s00382-008-0469-4

Dynamical changes in the ENSO system in the last 11,000 years

Anastasios A. Tsonis

Received: 12 June 2008 / Accepted: 11 September 2008 / Published online: 25 September 2008

Abstract A thorough analysis of a proxy El Nino/Southern Oscillation (ENSO) record indicates that a bifurcation occurred in the ENSO system sometime around 5,000 years B.P. As a result of this bifurcation the attractor became higher dimensional and a new mechanism of instability was introduced. As a consequence of these changes the system switched from a dynamics where the normal condition (La Nina) was dominant to a dynamics characterized by more frequent and stronger El Nino events.

Keywords ENSO · Climate variability · Chaos · Bifurcation

1 Introduction

It goes without saying that the El Nino/Southern oscillation (ENSO) phenomenon is one of the major players in climate. Its effects are worldwide and often devastating. Its properties and dynamics have been studied extensively using both models and observations. However, while models may point to interesting insights about ENSO variability over long timescales (see for example, Clement et al. 1998), observations are too limited to address this issue and thus to confirm model results. As such ENSO variability over millennia timescales is not well understood. Recently, proxy ENSO records have been constructed (Rodbell et al. 1999; Moy et al. 2002) thus providing an opportunity to study this variability. Here we employ the proxy ENSO data of Moy et al. 2002. This record (Fig. 1) is based on the distribution of inorganic clastic laminae in a core retrieved from Lake Laguna Pallcacocha in Ecuador. The laminae are deposited during ENSO-driven episodes of alluvial deposition in the Laguna Pallcacocha drainage basin. These laminae are mixed with dark-coloured organic-rich silt. The surface of the core sections was scanned and the intensity of the red colour was used to generate the proxy record. Then an age model was applied to create a yearly time series of events from 11,000 calendar years B.P. to today. According to the record, from 11,000 B.P. to about 5,000 B.P. the normal state (La Nina; low red colour intensity) is dominant, whereas in the last 5,000 years a switch to more frequent and strong El Nino events (high red colour intensity) has taken place. In a wavelet analysis of this data (Fig. 2; Moy et al. 2002) this shift is indicated by the collapse of two pre-5,000 years B.P. narrow bands above and below a period of 2,048 years into one broader band centered at period 2,048 years. Moy et al. 2002 suggest that this shift was due to changes in boreal summer insolation, a suggestion supported by a modeling study using the Zebiak and Cane ENSO model (Clement et al. 1998). Moy et al. 2002 interpreted this change as a shift from one periodic to another periodic state. However, as we will show here the nature of this shift is much more complex.

2 Data analysis and results

Because the shift occurred some time 5,000 years BP we split the record into two parts; the first is the period 11,000–5,000 B.P. and second the period 5,000-present. The present analysis consists of three different approaches to

A. A. Tsonis (✉)
Department of Mathematical Sciences, Atmospheric Sciences Group, University of Wisconsin-Milwaukee, Milwaukee, WI 53201-0413, USA
e-mail: aatsonis@uwm.edu

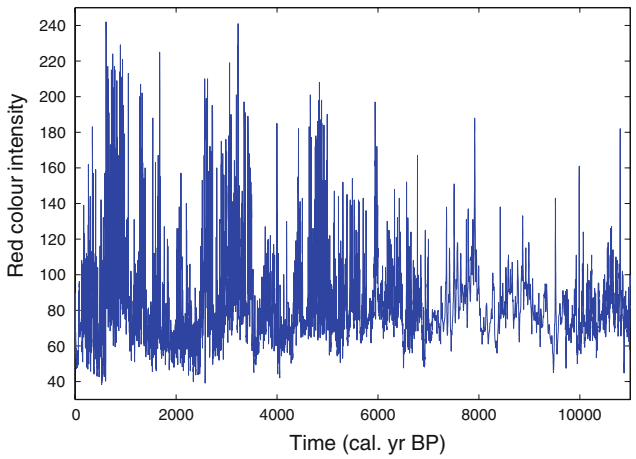

Fig. 1 The Moy et al. 2002 proxy ENSO record. Visual inspection of this record indicates that from 11,000 B.P. to about 5,000 B.P. the normal state (La Nina; low red colour intensity) is dominant, whereas in the last 5,000 years a switch to more frequent and strong El Nino events (high red colour intensity) has taken place

study nonlinear dynamics from observables embedded in some appropriate delay space. This embedding is achieved by considering a scalar time series $x(t)$ and its successive time shifts using an appropriate delay parameter τ (Packard et al. 1980; Ruelle 1981; Takens 1981). The first shift defines a 2-D embedding space [with coordinates $x(t)$, $x(t+\tau)$], the second shift defines a 3-D space [with coordinates $x(t)$, $x(t+\tau)$, $x(t+2\tau)$), and so on. At any embedding dimension n in our delay space, we have a cloud of points. Within this cloud we may find the number of pairs of points, $N(r,n)$, that are separated by a distance less than r. If we find that this number scales with r according to

$$N(r,n) \propto r^{d_2} \tag{2}$$

then the scaling exponent d_2 is the correlation dimension of the cloud of points for that n. Since the above equation is a power law, the value of d_2 is estimated by the slope of the plot $log\ N(r,n)$ versus log r. We then repeat this procedure and we check if d_2 reaches a saturation value D_2 as n increases. If this happens it would indicate that we have "locked" into the underlying attractor whose correlation dimension is D_2. Figure 3 shows the results when the Grassberger and Procaccia 1983a, b algorithm is used to estimate the correlation dimension for a delay $\tau = 6$ and embedding dimensions 2–9. More specifically (and more appropriately) it shows the slope, dlog $N(r,n)$/dlog r, versus log r plot [Tsonis 1992; Tsonis and Elsner 1995]. The idea is that if scaling exists, then dlog $N(r,n)$/dlog r is constant and independent of r; this constant manifesting itself as a plateau. From theory we know that a volume element in state space under the action of a chaotic flow will at first be pulled along the direction of greatest instability. This stretching, however, cannot occupy more and more volume (because the attractor is confined in a finite area in state space). The mechanism that prevents this is folding. Thus, the attractor has to fold onto itself. Successive iterations of this process result in the asymptotic attractor with folds within folds ad infinitum (i.e. a fractal object). It has by now been established that the proper τ is the one that emulates these properties of the attractor closely and that the effect of an increasing τ is also to pull nearby points apart (Tsonis 2007). Thus, the proper τ should be the one that results in the widest and best defined plateau. This can be easily assessed in a common procedure where the slope versus log r plot is produced by simultaneously varying the embedding dimension and delay parameter. Since the stretching and folding is a physical property, it may not relate well to statistical measures such as the autocorrelation function or mutual information, which were commonly used in the past to define τ. From our procedure we find that the best choice is $\tau = 6$.

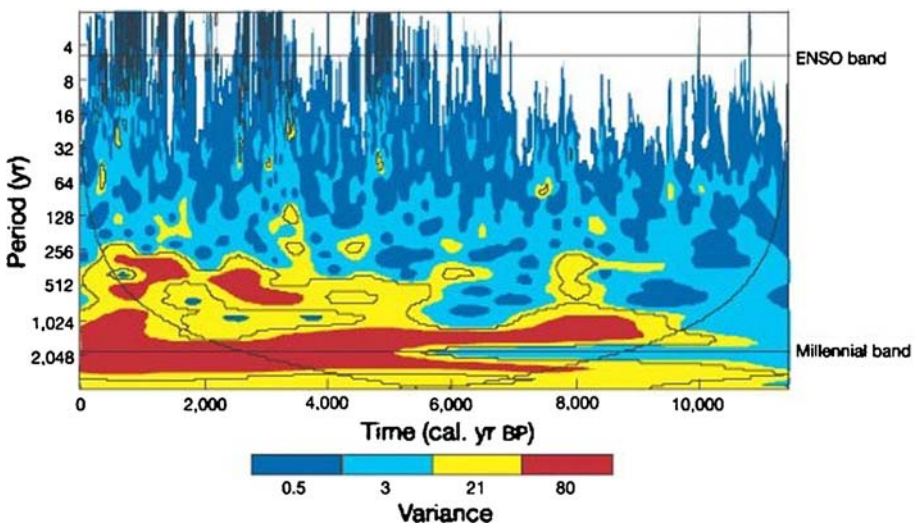

Fig. 2 A wavelet analysis of the record in Fig. 1 (from Moy et al. 2002). A major feature of this analysis is the collapse of two pre-5,000 years B.P. narrow bands above and below a period of 2,048 years into one broader band centered at period 2,048 years (Figure courtesy of Dr. Christopher Moy)

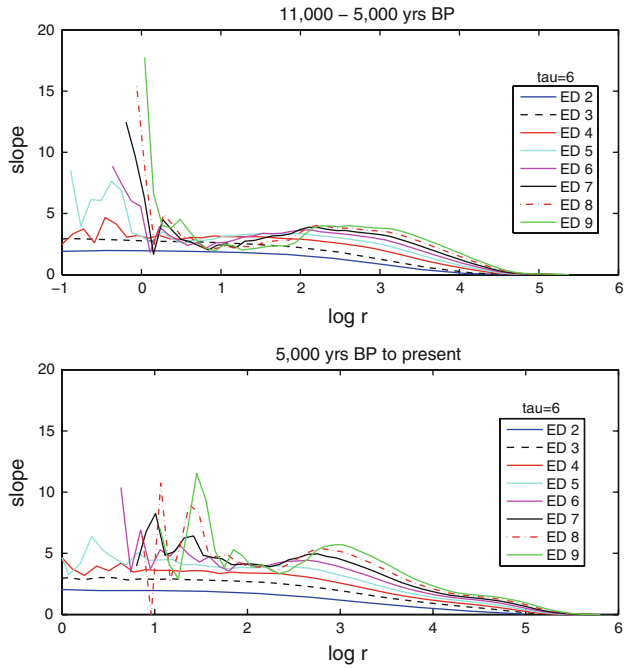

Fig. 3 Estimation of the correlation dimension for the two chosen periods. This figure indicates that the data in the first period are characterized by an attractor of dimension 3 and the data in the second period by an attractor of dimension slightly above 4 (see text for details)

The signature of the curves in Fig. 3 is exactly what we should observe from nonlinear dynamical systems. Assume that our attractor is a set of points in a two-dimensional space having a correlation dimension $D_2 \leq 2$. How does the slope versus log r plot would look like? For an embedding dimension of two, for scales smaller than the diameter of the attractor, the plot will show a plateau at slope = D_2. However, since the attractor has a finite diameter, for distances greater than this diameter $N(r,n)$ will reach a saturation value and will not change further with r. Because of that, the dlog $N(r,n)$/dlog r function (i.e. the slope) will tend to zero for very large r's. Now what will happen if we embed the data in three dimensions? In this case we distribute the points of the attractor into a much larger volume. The effect of this is that the density of points per unit volume decreases. Now, a pair in two dimensions separated by a distance r is separated by a longer distance. This "depopulation" results in poor statistics over small scales and manifests itself as fluctuations about the plateau. On the other end because we have embedded the attractor in a higher dimension than needed, the larger scales will appear higher dimensional than they actually are (much like when we curl a sheet of paper; the smaller scales remain planar but in large scales the sheet of paper appears three dimensional). Thus, when we embed the data in higher than needed dimensions, the local slope plot will show large fluctuations at very small scales, a plateau at intermediate scales at the level slope = D_2, a tendency for higher slope values at large scales (manifesting itself as a "hump"), and finally an approach to zero values for very large scales. The results in Fig. 3 are very consistent with this expected behavior and indicate a dimension of about 3 for the data in the first period (as indicated by the convergence at a common plateau at about slope ≈ 3 for embedding dimensions greater than two) and a dimension slightly over 4 for the data in the second period. These estimates comply with sample size requirements in the calculation of correlation dimensions. According to the Tsonis criterion the number of points necessary for the estimation of a correlation dimension D is $10^{(2+0.4D)}$. This has been verified with systems of known dimensions (Nerenberg and Essex 1990; Tsonis 1992; Tsonis et al. 1993, 1994). We thus conclude that the two periods are characterized by two different attractors. Further support for this is provided by surrogate data analysis. Figure 4 is similar to Fig. 3 but for surrogate data generated by inverting the observed spectra and randomizing the phases. Such procedures (Theiler et al. 1992; Schreiber and Schmitz 1996) preserve the autocorrelation function and power spectra of the original data set but not the dynamics and have been established as the proper way to test alleged dynamics. In this figure we do not observe any of the expected from dynamics structure nor do we observe any convergence at a common plateau. As the embedding dimension increases the plateau rises. This is the signature of random data not of dynamics. Random data fill any

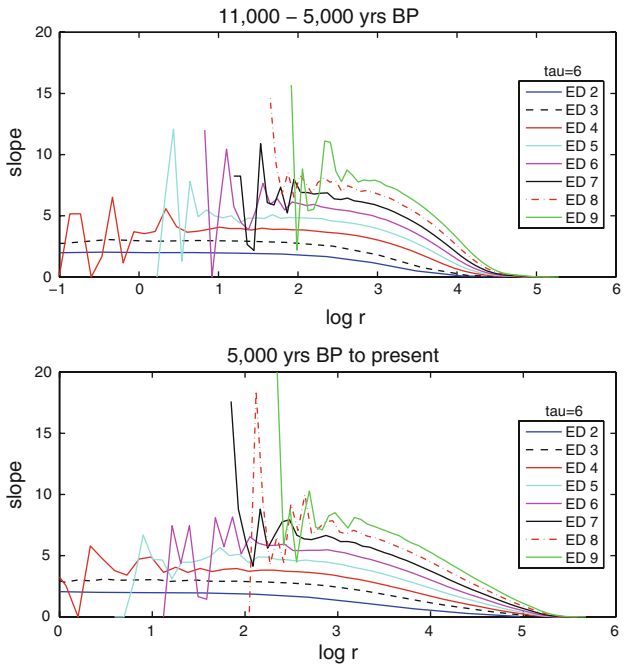

Fig. 4 Same as Fig. 3 but for random surrogate data. The convergence observed in Fig. 3 is absent here as expected from random data

embedding space uniformly thus their dimension is the dimension of the embedding space. Note that in the case of random data since no attractor exists, the estimated dimension may be progressively underestimated at high embedding dimensions but this may not be the case with data possessing low-dimensional attractors (Tsonis 1992; Tsonis et al. 1994).

Next we turn to the estimation of the Lyapunov exponents. The Lyapunov exponents measure the rate at which nearby trajectories converge or diverge. An n-dimensional attractor has n Lyapunov exponents. One is zero and the rest are positive or negative. Positive Lyapunov exponents indicate divergence of nearby trajectories (or stretching and folding), which is a property of chaotic attractors. Negative exponents indicate convergence of nearby trajectories and signify the fact that attractors usually have dimensions lower than the complete state space. For example the famous Lorenz (1963) system has a three dimensional state space but the attractor has a dimension slightly above two. This means that any set of initial conditions in a three dimensional cube must collapse onto a lower-dimensional attractor; hence there must be some "squeezing" of the original cube or a negative Lyapunov exponent. Once the data are embedded in the proper space we monitor the motion in that space of a point and also of points in its close neighborhood for some time called the decomposition length [Abarbanel et al. 1991; Brown et al. 1991]. From this monitoring one can estimate the Jacobian, which provides information about the Lyapunov exponents for a point (i.e. the local Lyapunov exponents). By repeating this procedure for many points we can obtain an average picture which will be related to the average Lyapunov exponents of the system. An embedding dimension of at least $2D_2$ is recommended for this procedure. Thus, we embed the data in the first period in a 7-dimensional space and of the second period in a 9-dimensional space using $\tau = 6$. Figure 4 shows the local Lyapunov exponents for 1,000 positions along the trajectory for a decomposition length of 200. We find that in the first period there is one positive, one zero and five negative Lyapunov exponents (in Fig. 5 only the first negative exponent is shown). For the second period we find two positive, one zero and six negative exponents. The presence of positive exponents indicates that the dynamics are chaotic. This is consistent with model results as well as of analysis of modern ENSO records (Elsner and Tsonis 1993; Tziperman et al.1994; Tsonis and Elsner 1996). It thus appears as if the bifurcation is not from one periodic attractor to another periodic attractor but from a chaotic attractor to a bigger chaotic attractor (this bifurcation is often referred to as explosive bifurcation). The variation of the local Lyapunov exponents with location is indicative of non-uniform chaotic attractors. Depending on the region in the attractor the

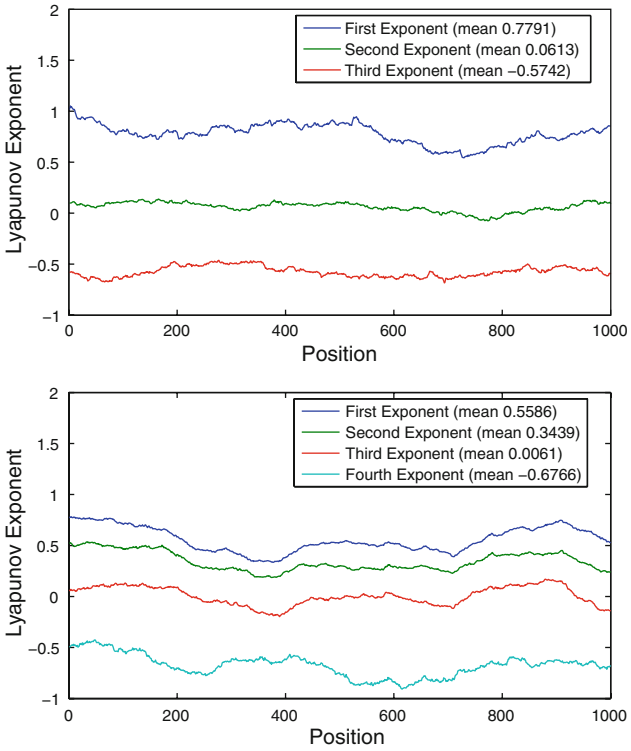

Fig. 5 Local Lyapunov exponents at 1,000 positions along the trajectory for the period 11,000–5,000 B.P. (*top*) and for the period 5,000 B.P.-present (*bottom*). The presence of positive exponents indicates that the dynamics are chaotic. Note that in the first period there is one positive exponent but in the second there are two positive exponents. This indicates that in the second period a new mechanism of instability has been introduced

divergence or convergence rate may be greater or smaller. The average values of the exponents suggest that indeed the dimension is low. According to Frederickson et al. 1983 these average values correspond to an information dimension (a measure close to the correlation dimension) of slightly above 3 and 4, respectively. Thus these results are consistent with the dimension estimates reported above. Moreover, they suggest that indeed some time about 5,000 years B.P. a bifurcation (change in the attractor) must have occurred as in the second period we now have two mechanisms of instability (corresponding to two positive Lyapunov exponents) rather than one. The inverse of the sum of the positive Lyapunov exponents defines the Kolmogorov entropy, a measure of predictability. Accordingly, predictability in the second period is lower than in the first period. This is consistent with latest results reporting that during El Nino events predictability decreases (Tsonis and Swanson 2008). It is worth noting here that the fact that we recover two positive Lyapunov exponents rules out the possibility that the underlying process is a random fractional Brownian motion (fBm). Such sequences may fool the procedure in producing a positive Lyapunov exponent

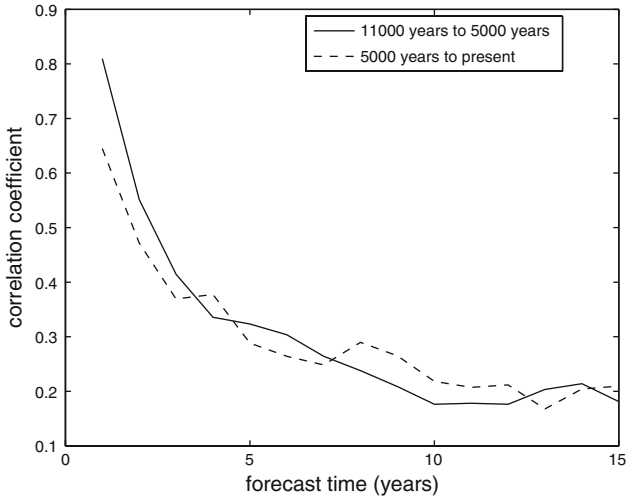

Fig. 6 Correlation coefficient between actual and predicted vales using nonlinear prediction. The loss of predictability as a function of prediction time also indicates chaotic dynamics

but they can never produce two positive Lyapunov exponents.

The above conclusions are further supported by nonlinear prediction. In nonlinear prediction once we have an appropriate embedding we can consider a terminal point and its close neighborhood. Then we can find the (local) linear mapping of the motion of its neighbors and extrapolate it to get a projection of the terminal point into the future (Farmer and Sidorowich 1987). The performance of nonlinear prediction is evaluated by estimating the correlation between predicted and actual values as a function of the prediction time step. Figure 6 shows the correlation between predicted and actual values as a function of prediction time using the nonlinear prediction algorithm of Wales 1991, which is based on the Farmer and Sidorowich 1987 local linear approximation approach. We see a decay of predictability with time; a feature consistent with chaotic dynamics (Sugihara and May 1990). We also observe that for short time steps predictability is better during the first period, which is consistent with the Kolmogorov entropy values calculated from the Lyapunov exponents. Note that this decay is not a power law, which according to the Tsonis–Elsner test (Tsonis and Elsner 1992) also rules out the possibility that what we are dealing here are random fractional Brownian motions, which are known to produce a small finite dimension when they are passed through the Grassberger–Procaccia algorithm for dimension estimation (Osborne and Provenzale 1989).

3 Conclusions

We have presented a variety of very consistent results from three different methods all of which point to the fact that the shift in the behavior of ENSO observed around 5,000 years B.P. is indeed a bifurcation. This bifurcation led to new dynamics. The attractor increased in size (it become higher dimensional), a new dominant mechanism of instability (a second positive Lyapunov exponent) was introduced, and the system changed from a dynamics where the normal condition (La Nina) was dominant to a dynamics characterized by more frequent and stronger El Nino events. As speculated by Moy et al. 2002 this may have been caused by changes in boreal summer insolation during that time. Such changes may have acted as an external parameter, which after reaching a critical value caused the system to bifurcate. Modeling suggests (Clement et al. 1998) that what could play the role of this parameter are easterly wind anomalies, which amplify during an increase in insolation (in early Holocene) and lead the system toward the La Nina state. On the other hand it is plausible that the new mechanism of instability in the second period could have been introduced from the slow changes in ocean dynamics, which are known to be affected during interglacial event. Our results thus provide new insights and challenges in the ongoing endeavor to understand the dynamics of this important mode of variability of the climate system at long timescales. At the same time they highlight the importance of proxy paleoclimate records as they continue providing important clues about climate variability at very long timescales.

Acknowledgments I thank the students in my spring 2008 class "nonlinear time series analysis" for helping me with the production of some of the figures used here.

References

Abarbanel HDI, Brown R, Kennel MB (1991) Lyapunov exponents in chaotic systems: their importance and their evaluations using observed data. Mod Phys Lett B 5:1347–1375

Brown R, Bryant P, Abarbanel HDI (1991) Computing the Lyapunov spectrum of a dynamical system from observed time series. Phys Rev A 43:2787–2806. doi:10.1103/PhysRevA.43.2787

Clement AC, Seager R, Cane MA (1998) Suppression of El Nino during the mid-Holocene by changes in the Earth's orbit. Paleoceanography 15:731–737. doi:10.1029/1999PA000466

Elsner JB, Tsonis AA (1993) Nonlinear dynamics established in the ENSO. Geophys Res Lett 20:213–216. doi:10.1029/93GL00046

Farmer JD, Sidorowich JJ (1987) Predicting chaotic time series. Phys Rev Lett 59:845–848. doi:10.1103/PhysRevLett.59.845

Frederickson P, Kaplan E, Yorke E, Yorke J (1983) The Lyapunov dimension of strange attractors. J Differ Equ 49:185–192. doi:10.1016/0022-0396(83)90011-6

Grassberger P, Procaccia I (1983a) Characterization of strange attractors. Phys Rev Lett 50:346–349. doi:10.1103/PhysRevLett.50.346

Grassberger P, Procaccia I (1983b) Measuring the strangeness of strange attractors. Physica D 9:189–208. doi:10.1016/0167-2789(83)90298-1

Lorenz EN (1963) Deterministic nonperiodic flow. J Atmos Sci 20:130–141. doi:10.1175/1520-0469(1963)020<0130:DNF>2.0.CO;2

Moy CM, Seltzer GO, Rodbell DT, Anderson DM (2002) Variability of El Nino/Southern Oscillation activity at millennial timescales during the Holocene epoch. Nature 420:162–165. doi:10.1038/nature01194

Nerenberg MAH, Essex C (1990) Correlation dimension and systematic geometric effects. Phys Rev A 42:7065–7074. doi:10.1103/PhysRevA.42.7065

Osborne AR, Provenzale A (1989) Finite correlation dimension for stochastic systems with power-law spectra. Physica D 35:357–381. doi:10.1016/0167-2789(89)90075-4

Packard NH, Crutchfield JD, Shaw RS (1980) Geometry from a time series. Phys Rev Lett 45:712–716. doi:10.1103/PhysRevLett.45.712

Rodbell DT et al (1999) A 15, 000-year record of El Nino-driven alluviation in southwestern Ecuador. Science 291:516–520. doi:10.1126/science.283.5401.516

Ruelle D (1981) Chemical kinetics and differentiable dynamical systems. In: Pacault A, Vidal C (eds) Nonlinear phenomena in chemical dynamics. Springer-Verlag, Berlin, pp 57–72

Schreiber T, Schmitz A (1996) Improved surrogate data for nonlinearity tests. Phys Rev Lett 77:635–638. doi:10.1103/PhysRevLett.77.635

Sugihara G, May RM (1990) Nonlinear forecasting as a way of distinguishing chaos from measurement error in time series. Nature 344:734–741. doi:10.1038/344734a0

Takens F (1981) Detecting strange attractors in turbulence. In: Rand D, Young LS (eds) Dynamical systems and turbulence, lecture notes in mathematics, vol 898. Springer-Verlag, Berlin, pp 366–381

Theiler J, Eubank S, Longtin A, Galdrikian B, Farmer JD (1992) Testing for nonlinearity in time series: the method of surrogate data. Physica D 58:77–94. doi:10.1016/0167-2789(92)90102-S

Tsonis AA (1992) Chaos: from theory to applications. Plenum, NY

Tsonis AA, Elsner JB (1992) Nonlinear prediction as a way of distinguishing chaos from random fractal sequences. Nature 358:217–220. doi:10.1038/358217a0

Tsonis AA, Elsner JB, Georgakakos KP (1993) Estimating the dimension of weather and climate attractors: Important issues about the procedure and interpretation. J Atmos Sci 50:2549–2555. doi:10.1175/1520-0469(1993)050<2549:ETDOWA>2.0.CO;2

Tsonis AA, Triantafyllou GN, Elsner JB (1994) Searching for determinism in observed data: a review of the issues involved. Nonlinear Process Geophys 1:12–25

Tsonis AA, Elsner JB (1995) Testing for scaling in natural forms and observables. J Stat Phys 81:869–880. doi:10.1007/BF02179296

Tsonis AA, Elsner JB (1996) Global temperature as a regulator of climate predictability. Physica D 108:191–196. doi:10.1016/S0167-2789(97)82013-1

Tsonis AA (2007) Reconstructing dynamics from observables: the issue of the delay parameter revisited. Int J Bifurcat Chaos 17:4229–4243. doi:10.1142/S0218127407019913

Tsonis AA, Swanson KL (2008) Topology and predictability of El Nino and La Nina network. Phys Rev Lett 100: 228502

Tziperman E, Stone L, Cane MA, Jarosh H (1994) El Nino chaos: overlapping resonances between the seasonal cycle and the Pacific ocean-atmosphere oscillator. Science 264:72–74. doi:10.1126/science.264.5155.72

Wales DJ (1991) Calculating the rate of loss of information from chaotic time series by forecasting. Nature 350:485–488. doi:10.1038/350485a0